

pores, and in a number of theoretical studies the effect of the size of the pores on their mobility has been investigated in detail. In general these studies show that the mobility of pores increases rapidly with a decrease in their size. Depending upon the mechanism postulated, the velocity is computed to be inversely proportional to the third or fourth power of the radius of the pore. Since fine pores can be obtained only with fine powders and since high mobility of pores will inhibit discontinuous grain growth, this establishes the great importance of the sizes of fine particles if high densities are sought in sintered materials.

Quite recently, Anderson and Jorgensen (15) have exploited the importance of decreasing the mobility of grain boundaries to produce pore-free yttrium oxide (Fig. 1). Pore-free aluminum oxide is not transparent because the individual grains are doubly refracting, and each grain boundary is a light-scattering interface. Yttrium oxide is cubic, and optically isotropic, so that the polycrystalline ceramic is as transparent as glass, with the additional advantage of good transmission in the infrared and a melting point of 2400°C.

Future Trends

Only a partial view of the importance of ceramics in today's technology and of the existing knowledge of the behavior of ceramic materials has been possible in this brief review. Much of the emphasis here, and by ceramists generally, has been to understand the thermodynamics, kinetics, and mechanisms of the structure-controlling reactions used for processing powders, because such understanding is necessary in order to regulate the processing. As new materials and new structures are needed, emphasis will shift to other methods—direct solidification from the melt and vapor-deposition techniques, for example. In the fabrication of products from powder, more attention will be paid to the control and characterization of the powder.

The need is for even more extreme properties—higher thermal conductivity coupled with low electrical conductivity, lower evaporation rates at high temperatures under reducing conditions, higher strengths, higher stiffness, higher electrical breakdown strength, and so forth. Some of these goals will be met by using materials that have not yet

been exploited to any great extent, but many of them will be met by minor modifications of the structure and composition of materials already well known. The future progress of ceramic science will be to provide the knowledge and understanding of this class of materials which will support these developments.

References and Notes

1. See, for example, AIME symposium on gas bubbles in solids, *J. Metals* **20**, 3a (1968).
2. J. Smit and H. P. J. Wijn, *Ferrites* (Wiley, New York, 1959).
3. A. Kelly, *Sci. Amer.* **217**, 160 (Sept. 1967).
4. W. B. Hillig, *J. Appl. Phys.* **32**, 741 (1961).
5. W. C. Loudon and K. Schmidt, *Illum. Eng.* **60**, 696 (1965).
6. W. Rhodes and R. E. Carter, *J. Amer. Cer. Soc.* **49**, 244 (1966).
7. H. S. Spacil, in preparation.
8. Y. F. Yu Yao and J. T. Kummer, *J. Inorg. Nuc. Chem.* **29**, 2453 (1967).
9. G. C. Kuczynski, *Trans. AIME* **185**, 169 (1949).
10. W. D. Kingery and M. Berg, *J. Appl. Phys.* **26**, 1206 (1955).
11. R. L. Coble and J. E. Burke, in *Progress in Ceramic Science*, J. E. Burke, Ed. (Pergamon Press, Oxford, 1963), vol. 3, p. 238.
12. C. Zener and C. S. Smith, *Trans. AIME* **175**, 15 (1949).
13. K. T. Aust and J. W. Rutter, in *Recovery and Recrystallization of Metals* [Interscience (Wiley), New York, 1963].
14. P. J. Jorgensen, *J. Amer. Cer. Soc.* **48**, 207 (1965).
15. ——— and R. C. Anderson, *ibid.* **50**, 533 (1967).
16. I thank A. Holik, E. Raviola, and J. Stafford for preparing several of the photomicrographs.

Hydrodynamic Studies of Structure of Biological Macromolecules

Experimental and theoretical advances yield structural details of proteins, DNA, viruses, and polysomes.

Victor A. Bloomfield

Hydrodynamic measurements have been prime sources of information on the molecular weight, size, shape, and configurational mobility of biological macromolecules. The quantities measured typically include sedimentation and translational diffusion coefficients, rotational diffusion coefficients, and intrinsic viscosities. Each such measurement gives a single number. Thus, even if all currently known or conceivable

hydrodynamic techniques were brought to focus on a single protein or nucleic acid molecule, the handful of parameters thereby obtained would be grossly inadequate to determine the thousands of atomic positions in the molecule. For atomic details, only x-ray diffraction studies will suffice. However, hydrodynamic studies are extremely useful for elucidating overall, long-range aspects of biopolymer structure.

This article reviews some of the developments which have forged hydrodynamics into a sharper and stronger tool for the study of biopolymer structure. The greatest experimental advances have been made in ultracentrifugation, where improved optical systems and density-gradient techniques have enabled measurements of a precision, sensitivity, and diversity never before possible. Viscometry, long a key technique in the characterization of synthetic polymers, has been adapted to the very low shear stress situations necessary for studying DNA of high molecular weight. Methods for the study of rotational motion and relaxation, notably fluorescence depolarization and flow and electric birefringence, have provided insight into the dynamical behavior of proteins and nucleic acids.

Concurrent with the experimental advances has come a flurry of significant theoretical activity. The number of types of model structures in terms of which hydrodynamic experiments can be interpreted has expanded sub-

The author is assistant professor of physical chemistry at the University of Illinois, Urbana.

stantially. In addition to the standard ellipsoids of revolution and flexible random-coil models for macromolecular structure, we can now deal with macromolecules composed of complicated assemblies of subunits and with semiflexible, wormlike chains. The predicted behavior of these more complicated model structures, when combined with electron microscopic studies of biopolymer morphology and topology, leads to the interpretation of experiments in terms of structural parameters pertinent to the real molecule in solution. Recent theoretical developments have also elucidated the effect of some of the approximations which enter these model calculations.

Finally, we review the application of these techniques and theories to several types of biological macromolecules. These applications include: the study of subunit structure and association and allosteric changes in proteins; determination of the molecular weight and flexibility of native DNA, and study of the structure of cyclic and supercoiled DNA; study of the size and structural transitions of bacteriophages; and characterization of the conformation of polysomes in solution.

Ultracentrifuge Techniques

In the past few years the common schlieren optical system for the ultracentrifuge (1) has been supplemented or supplanted for many applications by interference and absorption optical systems. The Rayleigh interference optical system (1, 2) produces a displacement of interference fringes formed by slits placed behind a sedimenting solution column and a reference solvent column. The fringe displacement is directly proportional to the difference in refractive index, and hence concentration, between solution and solvent; it can be measured with great accuracy. The number and movement of the sedimenting boundaries are not as conveniently visualized as with the schlieren system, which gives the refractive index gradient directly. However, the interference system gives very much greater accuracy in the determination of concentrations, and allows study of somewhat more dilute solutions. It has been widely used for the determination of molecular weights in sedimentation equilibrium, and shows promise for the study of preferential binding of small molecules to macromolecules.

The domains of DNA molecules of

high molecular weight are so large that it is necessary to measure sedimentation coefficients at very low concentrations, where refractive index methods are inapplicable. This has been done by reviving (3) the absorption optical system used by Svedberg (4) in his initial work with the ultracentrifuge. By using the strong nucleotide absorption around 260 $m\mu$, it was possible to lower the minimum feasible concentration from the 0.1 g/100 ml attainable with schlieren optics to 1 mg/100 ml. This extreme sensitivity can also be used for study of dilute solutions of proteins and of interacting systems (5). Although photographic recording of the cell image, with densitometric analysis of the films, has been employed most widely, photoelectric scanning systems have been developed (5) and are commercially available. These have the marked advantage of allowing the run to be followed while it is in progress.

A very ingenious method for studying the sedimentation of active enzymes has been devised by Cohen (6). A minute amount of enzyme solution, at a concentration in the micrograms per milliliter range, is layered on a substrate solution. As the thin enzyme layer sediments, its motion is followed by observing spectrophotometrically the disappearance of substrate or appearance of product.

One of the most important advances in analytical ultracentrifuge practice is the band centrifugation technique of Vinograd *et al.* (7). An adaptation of the zone centrifugation technique in the preparative ultracentrifuge (8), this involves layering a thin lamella of a macromolecule solution onto a denser liquid in a rotating ultracentrifuge cell. A density gradient, which stabilizes the system against convection, is generated during the experiment by the diffusion of small molecules under the combined influence of the centrifugal field and the difference in their chemical potential in the polymer solution and in the sedimentation solvent. Band centrifugation has a number of significant advantages, among which are the small amounts of material required, the physical separation of resolved components in a mixture, and the leaving of slow-moving contaminants behind the moving bands. In conjunction with the absorption optical system, this technique has been very widely used in nucleic acid studies. A substantial amount of work has been done on band-forming centerpieces (9), suitable solvent systems (10), and detailed the-

oretical interpretation of band patterns (9, 11).

Interpretation of sedimentation experiments demands a knowledge of the polymer partial specific volume \bar{v}_2 , since the sedimentation coefficient S is related to the molecular weight M_2 and translational frictional coefficient in two-component systems by

$$S = M_2(1 - \bar{v}_2\rho)/N_A f \quad (1)$$

where N_A is Avogadro's number and ρ is the solution density. Standard methods, mainly pycnometric, are available for determining \bar{v}_2 (12). However, these require relatively large amounts of material, which may be difficult to obtain for many biologically interesting substances. Sedimentation equilibrium experiments give the buoyant molecular weight $M_2(1 - \bar{v}_2\rho)$ directly. By performing equilibrium experiments in H_2O - D_2O mixtures, and by plotting $M_2(1 - \bar{v}_2\rho)$, versus ρ , one can determine simultaneously both M_2 and \bar{v}_2 (13). This technique, though not of highest accuracy, requires only small amounts of material, and purity requirements are not stringent.

Viscosity and Rotatory Motion

Viscometry has long been one of the prime methods for characterizing high polymers in solution. A difficulty arises in application to DNA of high molecular weight because of its extreme sensitivity to distorting shear stresses. This makes the intrinsic viscosity at shear rates commonly found in capillary viscometers (10^3 per second) much lower than that characteristic of the molecule in the limit of zero shear. Specially designed capillary viscometers (14) produce shear rates of about 10 per second, but even these are inadequate for very high molecular weight viral and bacterial DNA.

A viscometer now in wide use which obviates this difficulty is the all-glass rotating cylinder viscometer designed by Zimm and Crothers (15). This features an inner rotating cylinder which is driven by a hysteresis interaction between a small iron plug in the rotor bottom and an external rotating magnetic field. The rotor is supported by buoyancy and centered by surface tension. Shear rates as low as 10^{-2} per second, corresponding to shear stresses in aqueous solution of 10^{-4} dyne/cm², are possible with this instrument; and it has been shown that the intrinsic viscosities of viral DNA's with molecu-

lar weights as high as 1.3×10^8 measured thereby are effectively zero shear viscosities.

Among the difficulties associated with the use of the Zimm-Crothers (15) viscometer are the inability to change shear rates without changing rotors when studying non-Newtonian effects, the need for extreme surface cleanliness, and the relatively large volumes of solution (about 3 ml) needed. These difficulties have been overcome in a rotating Cartesian-diver viscometer designed by Gill and Thompson (16). The rotor is driven by the interaction of a rotating magnetic field with a magnetic field caused by eddy currents induced in a conducting ring in the bottom of the rotor. It is kept submerged at constant depth by a servomechanism-controlled pressure-regulating system. Despite somewhat greater complexities of construction, this viscometer is versatile and easy to use, and will probably become the instrument of choice for DNA work.

Automatic recording of rotor rotation speed has been developed (17) which makes viscosity measurements more convenient and, with appropriate electronic circuitry, allows viscometric study of kinetics.

Rotational motion and relaxation can be studied by a number of techniques, all of which are sufficiently complex as not to be in wide use. However, there have been a number of developments in instrumentation recently, and it is hoped that the great potential of these techniques for studying asymmetry and relaxation behavior can be vigorously exploited.

Perhaps the most common of these techniques is flow birefringence, in which the macromolecules are oriented by flow, usually between concentric cylinders (18). A photoelectric detection system has been designed that is substantially more sensitive than the standard optical compensation system (19), which makes it possible to study low concentrations of DNA of high molecular weight. By rapidly braking the rotor, it is possible to study polymer relaxation times (20). An apparatus has also been constructed which permits measurement of birefringence and dispersion in the radial as well as axial direction (21). It is thereby possible to completely determine the refractive index ellipsoid of the streaming fluid.

Orientation in flow can also be studied by flow dichroism (22).

Macromolecules may be oriented by strong electric fields, and the solu-

tion anisotropy may be studied by dichroism or birefringence measurements. This technique can provide information on the rotational diffusion coefficient and internal rigidity of the polymer, its dipole moment and polarizability, and its interaction with the surrounding ion atmosphere. For interpretation of experiments, however, the separate contribution of each of these parameters must be understood theoretically, a task which is rather far from completion. An important instrumental development in this field is the introduction of a high-speed delay line pulse generator (23) which enables the study of globular proteins as well as long, asymmetric polymers. Relaxation times may be studied by electric birefringence relaxation (24).

Polymer orientation in an electric field may also be studied by dielectric dispersion (25). The relaxation times of large, asymmetric polymers are long—in the millisecond range or longer—and therefore problems of electrode polarization in conducting solutions at the requisite low frequencies are severe. However, progress in this area has been made recently (26), and a variety of relaxation times have been observed in solutions of proteins, synthetic polypeptides, and nucleic acids.

We may finally mention fluorescence depolarization as a very useful method of studying rotation and conformational flexibility in proteins. Although the lifetimes of the fluorescent amino acids are themselves too short to be very useful in the study of rotation relaxation, fluorescent conjugates may be made which have lifetimes in the proper range and other desirable properties. The theory and applications of this technique have been the subject of several recent reviews (27).

Basic Hydrodynamic Principles

The treatment of viscous flow most frequently encountered is based on the Navier-Stokes equation. An alternative treatment was developed by Oseen (28) and adapted for macromolecular suspensions by Burgers (29). This approach concentrates on the motion of a fluid produced by the application of forces to points in the fluid. This formulation is obviously appropriate and convenient for calculation of the hydrodynamic behavior of chain molecule solutions. The polymer segments may be identified with the points at which force is being applied to the solvent

due to the relative motion of solvent and segment.

One may write that the force \mathbf{F}_i on the solvent flowing with velocity \mathbf{v}_i at the position of a segment moving with velocity \mathbf{u}_i is

$$\mathbf{F}_i = -\zeta(\mathbf{v}_i - \mathbf{u}_i) \quad (2)$$

ζ is the translational frictional coefficient of a segment, which for a sphere of radius r in a solvent of viscosity η_0 is, according to Stoke's law, $6\pi\eta_0 r$.

The velocity \mathbf{v}_i is not the bulk solvent velocity \mathbf{v}^0 because of the perturbation of solvent flow by the motion of the other segments in the chain. This effect is called *hydrodynamic interaction*. We write the velocity at i as a sum of \mathbf{v}^0 and the perturbations due to all the other segments:

$$\mathbf{v}_i = \mathbf{v}^0 + \sum_{j \neq i} \mathbf{T}_{ij} \cdot \mathbf{F}_j \quad (3)$$

The hydrodynamic interaction tensor \mathbf{T}_{ij} is an operator which converts a force exerted on the solvent by the j th segment into a velocity perturbation at the position of the i th segment. It is a function of the vector distances \mathbf{r}_{ij} between pairs of segments. It is in this way that the polymer dimensions are brought into the problem.

A further factor which must be taken into account is Brownian motion. If the shear rates in the system are sufficiently low with respect to the rotational diffusion coefficients of the macromolecule, \mathbf{T}_{ij} may be taken as an average over all orientations of the molecule with respect to an external coordinate system. If, in addition, the polymer is flexible, it is necessary to average over all internal configurations of the chain. The result is that (30)

$$\langle \mathbf{T}_{ij} \rangle = (1/6\pi\eta_0) \langle 1/r_{ij} \rangle \quad (4)$$

where the angular brackets denote averaging over internal configurations.

Theoretical Results

The concepts outlined above were integrated by Kirkwood (31) into a theory of irreversible processes in solutions of macromolecules composed of identical subunits. The simplest application is to the translational frictional coefficient f in Eq. 1. The total force \mathbf{F} exerted by the macromolecule on the solvent is the sum of the forces exerted by the subunits:

$$\mathbf{F} = \sum_i \mathbf{F}_i \quad (5)$$

It is also equal to the product of f and the relative velocity of the macromolecular center of mass with respect to bulk solvent:

$$\mathbf{F} = -f(\mathbf{v}^0 - \mathbf{u}) \quad (6)$$

Solution of the set of simultaneous Eqs. 2 and 3, and use of Eqs. 4 to 6, with $\mathbf{u}_i = \mathbf{u}$, then yields

$$f = N\xi / \left[1 + (\xi/6\pi\eta_0 N) \sum_{i \neq j} \sum_{j} \langle 1/r_{ij} \rangle \right] \quad (7)$$

N is the number of subunits. If the double sum were missing from the denominator of Eq. 7, the frictional coefficient of the polymer would be the sum of the frictional coefficients of the monomers. This is the so-called "free-draining" limit. The presence of the double sum reflects hydrodynamic interaction, which lowers f because solvent is trapped to a certain extent within the polymer domain and moves with it through solution.

Equation 7 has been used to calculate f for a wide variety of macromolecules for which dimensions or dimensional statistics are known, so that $\langle 1/r_{ij} \rangle$ may be evaluated. Some results for biological macromolecules are discussed below. Results are surprisingly accurate even for short-chain hydrocarbons, except when the solvent molecules are substantially larger than the polymer segments (32). This supports the validity of the assumption that the solvent may be treated as a hydrodynamic continuum.

A similar treatment is applicable to rotational motion. The Kirkwood theory (31) has been applied by Hearst (33) to calculate the components of the rotational diffusion coefficient tensor \mathbf{D} for a distribution of elements having cylindrical symmetry. The result has been used, with appropriate chain statistics, to calculate the diffusion coefficients of wormlike coils and weakly bending rods, which are good models for long and short-chain double-helical DNA.

The theory outlined above has been generalized by Bloomfield and co-workers (34) to accommodate structures composed of assemblies of nonidentical subunits. The subunits are modeled by surface shells of smaller spheres of identical size. In the limit of a continuous surface distribution, this "shell model" approach was shown to give exact results in translation and rotation for a sphere, and to deviate by only a few percent from the results for

ellipsoids of revolution. The analog of Eq. 7 for an assembly of spherical subunits of differing radii r_i is

$$f = 6\pi\eta \left(\sum_i r_i^3 \right)^2 / \left[\sum_i r_i^3 + \sum_{i \neq j} \sum_j r_i^2 r_j^2 \langle 1/r_{ij} \rangle \right] \quad (8)$$

This approach lends itself well to computer calculations of frictional properties of rigid macromolecules of complex shape. The double summation in Eq. 8 is evaluated numerically after the disposition of subunits has been established.

Although the Kirkwood (31) theory of irreversible processes may be used for the calculation of intrinsic viscosity $[\eta]$, a more convenient method has been found. This method, which was introduced by Rouse and by Bueche (35), employs the familiar device of normal coordinates. Zimm (36) managed to solve the eigenvalue problem for a Gaussian chain with hydrodynamic interaction. The beads in the polymer chain move under the combined influence of direct pulls exerted by their nearest neighbors along the chain, Brownian motion, and frictional resistance of the solvent as modified by hydrodynamic interaction. The resultant intrinsic viscosity is a sum of contributions from each of the normal modes.

The Zimm result could be cast in the form proposed by Flory (37),

$$[\eta] = \Phi \langle L^2 \rangle^{3/2} / M \quad (9)$$

where M is the polymer molecular weight and $\langle L^2 \rangle$ the mean-square end-to-end distance of the chain. The parameter Φ was calculated to have the value 2.84×10^{23} cgs units in a theta solvent, in which there are no net excluded volume effects, so that polymer chains have their ideal random-walk dimensions. Subsequent calculations (38) have shown that Φ is a decreasing function of excluded volume, in accord with experiment, and is about 2.1×10^{23} in typical good solvents.

For stiff-chain molecules such as wormlike coils, it is necessary to take bending modes into account. Harris and Hearst (39) have made such a calculation, using Green's function techniques to calculate the eigenvalues and eigenfunctions in the free-draining limit, and using perturbation theory to pass from these results to the zero-frequency viscosity in the presence of

hydrodynamic interaction and excluded volume.

Mention should also be made of the useful approximate theory of intrinsic viscosity devised by Peterlin (40). This theory simplifies the polymer normal modes by assuming that segments related symmetrically on either side of the middle of the chain move with equal and opposite velocities. The velocity of a segment is linearly related to its contour distance from the chain center. Agreement with exact theories (36) is good, which bolsters confidence in the applicability of the Peterlin theory to complicated situations in which exact solutions cannot be obtained.

There are three approximations in the theory outlined above which have drawn attention. The first is the premature averaging of the Oseen interaction tensor implicit in the combination of Eqs. 3 and 4. Fixman and Pyun (41) have recalculated the intrinsic viscosity of flexible chains by a procedure which avoids this approximation. The avoidance of preaveraging leads to a 5 percent reduction in Φ of Eq. 9, to 2.68×10^{23} in a theta solvent. This approximation is therefore not serious. Ishihara (42) has also developed a method of calculating frictional properties without preaveraging the Oseen tensor, but this method has not as yet been combined with a detailed treatment of chain dynamics.

The second approximation is the representation of monomers as point sources of friction. For a rigid rodlike polymer, it has been shown (43) that this approximation can lead to singularities in the translational diffusion coefficient for physically plausible values of hydrodynamic interaction.

Finally, it has been noticed that Kirkwood's derivation of Eq. 7 is not exact (44). Among other things, this has the disturbing consequence that the diffusion coefficients of a long rigid rod and a rigid ring of the same length are equal, though physical intuition would suggest that the latter would have a larger \mathbf{D} because of its more compact shape. Even more disturbing is the fact that when the exact result for the ring is used (44, 45), it is found that $\mathbf{D}(\text{ring}) < \mathbf{D}(\text{rod})$. This paradox may be related to the inadequacies in the Oseen approximation noted in the preceding paragraph.

Since calculations based on the Oseen approximation have proved adequate for flexible chains and rigid arrays which are not too asymmetric (34), it may be conjectured that the approxi-

mation will in general be satisfactory for configurations of approximately spherical symmetry. It is clearly important to investigate this point further.

Protein Subunits

The experimental and theoretical advances described above have led to substantial advances in our understanding of the structure of biological macromolecules in solution. The subunit structure of proteins is one such area of increased understanding.

Bovine serum albumin undergoes a reversible transition below pH 4 which is attended by large changes in hydrodynamic properties but not by a change in molecular weight. Intrinsic viscosity increases, and diffusion and sedimentation coefficients decrease, suggesting an overall expansion of the molecule; but fluorescence depolarization increases (46), suggesting a decrease in size of the rotationally relaxing unit. These observations suggest that the transition involves a separation of covalently bonded subunits. This interpretation was supported by the finding that pepsin-catalyzed hydrolysis of bovine serum albumin in acid yielded subunits of molecular weight 30,000 and 11,000 to 12,000 (47). Detailed calculation of hydrodynamic and low-angle x-ray scattering properties of various subunit models led to the proposal of a linear trimer model, which contains one spherical subunit of 26.6-Å radius and two subunits of 19-Å radius (48). Other interesting examples of the combination of hydrodynamic and chemical cleavage studies on the subunit structure of proteins are found in work on myosin (49) and γ -globulin (50).

Hemocyanins are multisubunit proteins whose structures may be observed by electron microscopy (51). The presumed hierarchy of structures is shown in Fig. 1, along with a comparison between observed sedimentation coefficients and those calculated from Eqs. 1 and 8 by using the electron microscope dimensions of the 59S component of squid hemocyanin (52, 53). Agreement is excellent, and underlines the utility of a combination of hydrodynamics and electron microscopy in studying biopolymer structure.

Quantitative studies of the equilibrium and kinetics of reversibly associating systems of proteins or other macromolecules may also be carried out in the ultracentrifuge (54). For slow reactions, peaks corresponding to each of the separate components will be observed; while for reactions in which equilibrium lies far to one side, only the peak corresponding to favored species will be seen. If the equilibrium is very rapid, only one peak may be seen; but the apparent sedimentation coefficient will increase with concentration, because of the formation of heavier, faster-sedimenting aggregates (55). This is in contrast to the usual behavior for non-associating polymers, in which S decreases with concentration because of hydrodynamic interaction. Reactions of intermediate velocity may lead to very complex sedimentation patterns (54-56).

A cautionary note has been injected into sedimentation studies of association by the observation that the equilibrium constant for the myosin monomer-polymer system is highly pressure-dependent (57). Since hydrostatic pressure can vary by several hundred atmospheres from top to bottom of the cell, this effect may be very

important. Similar considerations obtain in sedimentation equilibrium (58).

Sedimentation velocity studies have demonstrated a structural change in the regulatory enzyme aspartyl transcarbamylase (59). In the presence of both carbamyl phosphate and the substrate analog succinate, the sedimentation coefficient of the enzyme dropped 3.6 percent. This is one of the few demonstrations of gross structural changes in allosteric enzymes.

DNA

The hydrodynamic behavior of linear double-helical DNA's of various molecular weights has been studied extensively over the past decade. Just as with common synthetic polymers, much of this work has been devoted to establishing correlations of S and $[\eta]$ with molecular weight. This enables both the determination of the molecular weight of an unknown DNA from measurement of S or $[\eta]$, and investigation of the characteristic structural parameters of the chain. These studies have been collated and summarized by Eigner and Doty (60) in Fig. 2. It will be noted that log-log plots of S versus M , and particularly $[\eta]$ versus M , are nonlinear, which is a consequence of the remarkable stiffness of the double helix.

The lines in Fig. 2 have been fit by the equations (61)

$$\log(S_{20,w}^0 - 2.7) = -1.819 + 0.445 \log M \quad (10)$$

$$\log([\eta] + 5) = -2.863 + 0.665 \log M$$

It has been possible (62) to rationalize these expressions, using the Kirkwood (31) and Peterlin (40) theories, if DNA is treated structurally as a wormlike coil (63) with excluded volume effects. The double helix is rodlike in the short run, behaves like a weakly bending rod over a contour length of several hundred angstroms, and acquires substantial flexibility over long contour lengths. It is this behavior which is characteristic of a wormlike coil.

The excluded volume parameter ϵ , defined by

$$\langle L^2 \rangle / \langle L^2 \rangle_0 = \sigma^\epsilon \quad (11)$$

where σ is the number of statistical segments in the chain and the subscript zero denotes a theta solvent, is 0.11. Of this, roughly half is attributable to polyelectrolyte repulsions, and the rest to physical excluded volume effects (64). The persistence length of

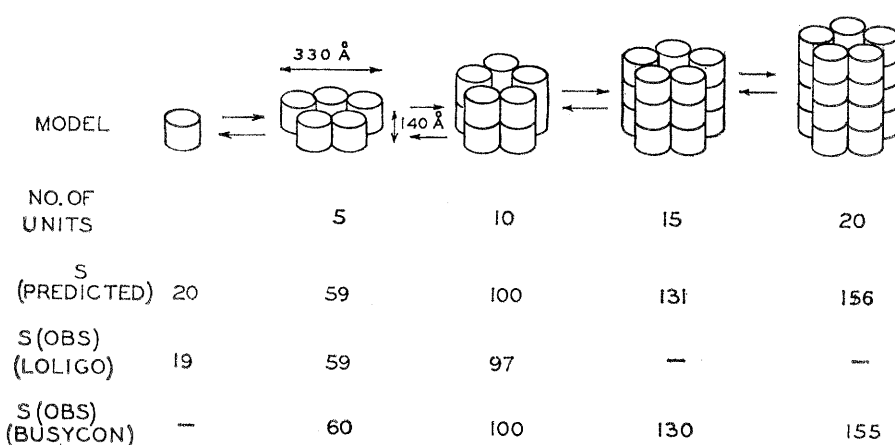


Fig. 1. Structures and sedimentation coefficients of molluscan hemocyanins. [Reproduced with permission from Bloomfield *et al.* (53)]

the wormlike coil—roughly speaking, the length of polymer backbone over which correlations with the initial direction of the chain decay to zero—lies between 270 and 450 Å from S and $[\eta]$ measurements (39, 62). This range is consistent with light scattering measurements (65), while flow birefringence gives an upper limit of 550 Å (66). The hydrodynamic diameter of the double helix is around 27 Å (62).

Circular DNA molecules have been detected in a large number of viruses, bacteria, and higher organisms (67). Theoretical calculations (62, 68) indicate that the ratio of the sedimentation coefficients of linear and circular polymers of the same molecular weight, S_L/S_C , should be about 0.88, nearly independent of excluded volume. This is observed experimentally. The ratio $[\eta]_L/[\eta]_C$ has been predicted (68) to begin at 1.55 for $\epsilon = 0$, and to increase with increasingly excluded volume. This has been verified experimentally (64), and indicates that, because their ends are tied together, circular molecules are less free to expand under the influence of excluded volume forces than are linear polymers.

Twisted circular DNA molecules have also been found in a variety of sources (67, 69). In this topologically very interesting type of molecule, superhelical turns are formed as the Watson-Crick double helix winds or unwinds. That is, opposite sides of the circular molecule become wrapped around each other in helical fashion. Sedimentation coefficient calculations (70) which model the twisted circular DNA as a rigid, rodlike superhelix give a number of superhelical turns in the same range—about 15 to 20—as observed experimentally (69). At ionic strengths below $10^{-2}M$, a model for twisted circular DNA which agrees qualitatively with experiment is a superhelix wound around a torus (70).

Plots of S versus molecular weight for circular and twisted circular DNA have been presented (71). However, Wang *et al.* (72) have shown that the amount of supercoiling is a function of temperature and ionic environment. Therefore, S versus M correlations for twisted circular DNA must be viewed with caution.

Viruses and Polysomes

Very complex virus structures may be observed in electron microscopy. A case in point is T2 bacteriophage, de-

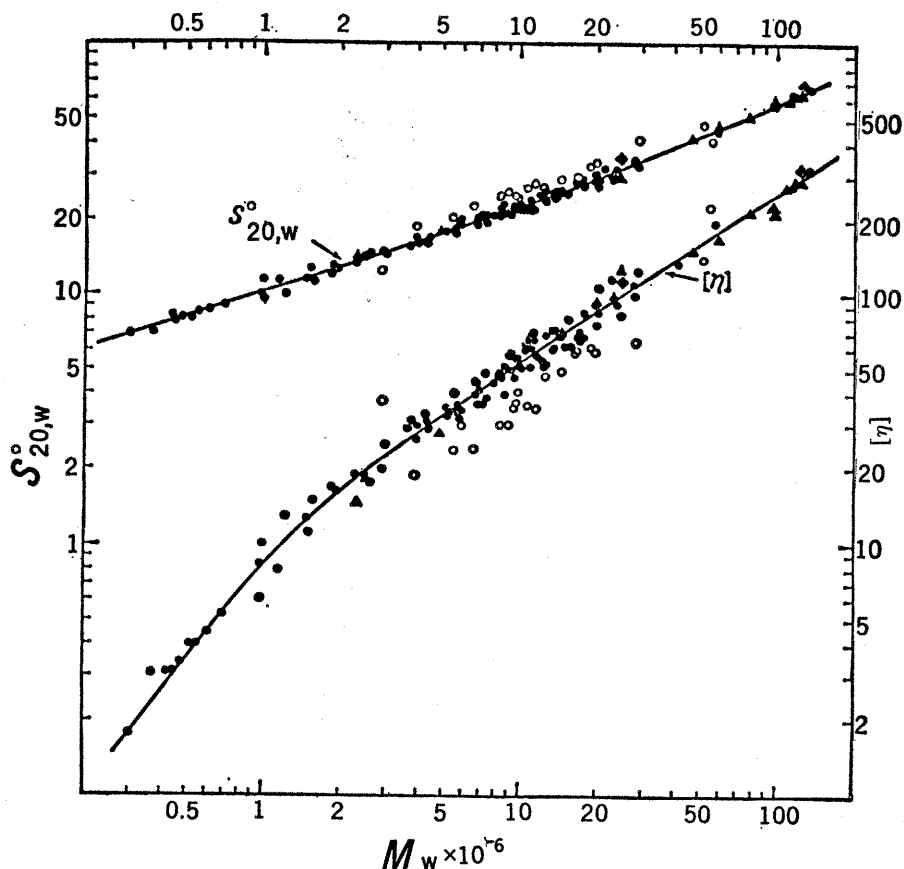


Fig. 2. Double-logarithmic plots of sedimentation coefficients and intrinsic viscosity versus molecular weight for native DNA. Experiments performed in 0.2M Na⁺ neutral buffer. [Reproduced with permission from Eigner and Doty (60)]

picted schematically in Fig. 3. It has a hexagonal bipyramidal head, a tail (actually a tail core and contractile sheath), a tail plate, and six kinked tail fibers (73). In addition, T2 undergoes a transition, triggered by decreasing temperature, decreasing pH, or increasing [Ca²⁺], from the “slow” form which comes out of the lysed bacterial host with a sedimentation coefficient of

700 S , to the “fast” form necessary for injection into a new host with a sedimentation coefficient of 1000 S (74). The rotational diffusion coefficients of the slow and fast forms, as measured by electrical birefringence, are 111 ± 22 per second and 555 ± 54 per second, respectively (75).

Considerable interest attaches to the nature of the structural changes in the virus giving rise to these large differences in hydrodynamic properties. It has been speculated that the change lies in extension of the tail fibers (75, 76), or in a difference in head permeability along with a small change in head size (77). Calculations based on Eqs. 7 or 8 for translation (53), or on equivalent shell model expressions for rotation (78), suggest that neither explanation is adequate. Instead, the slow form must have a head two or three times larger than the size observed in electron microscopy in order to account for the sedimentation and rota-

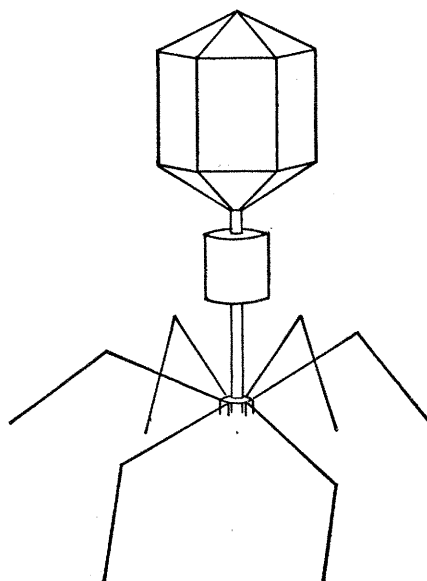


Fig. 3 (left). Structure of T2 bacteriophage, reproduced with permission from Filson (78). Kinks in the tail fibers, details of the tail core and sheath structure, and the tail plate were neglected in the calculations (53, 78).

tional diffusion data. Confidence in these calculations is buttressed by the finding that reaction of T2 with indole, which is presumed only to change the fiber disposition from an extended to a nonextended state, leads to an increase in S of 10 to 15 percent (79), in accord with theory (53).

However, macroscopic studies of the rotation of T2 phage models in highly viscous oil indicate that the tail fibers have substantially more effect than was indicated by the calculations reported above (80), so that the head size changes in going from the slow to the fast form need not be so large. This discrepancy may tentatively be ascribed to the failure of the Oseen approximation in the highly asymmetric structure depicted in Fig. 3. Doubt is also cast thereby on the interpretation of the indole-binding experiments (79).

Electron micrographs of polysome preparations often show polygonal or helical arrays. Determination of sedimentation coefficients of a series of polysomes from rat liver, containing from 1 to 12 ribosomes (81), afforded an opportunity to test whether such ordered configurations were present in solution. It was found (82), by using Eq. 7 with various assumed models for polysome structure, that helical or polygonal arrays were too compact, while random coil configurations, generated on lattices by complete enumeration or Monte Carlo computer techniques, were too extended. It appears, however, that essentially random configurations, with weak attractive interactions between the ribosomes, are the most likely. It is not clear whether the ordered structures seen in electron microscopy are preparational artifacts, or whether they have some functional significance in connection with the cell membrane.

Summary and Prospects

The advances in our knowledge of biopolymer structure reported above reflect a fourfold confluence of advances in experimental and theoretical techniques. Biologists and biochemists have made great strides in identifying, and isolating in forms sufficiently pure and undamaged to be profitably studied by physical methods, a whole host of multisubunit proteins, nucleic acids, viruses, and other complex structures. Physical chemists have developed sedimentation analysis, viscometry, and other instrumental techniques to a level of sensitivity and accuracy where they

can cope with the low concentrations and subtle changes encountered in these macromolecular systems. Electron microscopists have made possible the direct visualization of the larger biological macromolecules, thus extending our conceptions of structure and topology far beyond the simple models of the random coil and ellipsoid of revolution. Theoreticians have devised methods for calculating the properties of these more complex types of structures, thus enabling (with the help of computers) assessment of size and structure under conditions in solution closely approaching the physiological.

It seems clear that further pursuit of this fourfold way (a waterway, since we have been discussing hydrodynamics)—isolation, measurement, visualization, and calculation—will lead to further striking advances in our understanding of the structure of biological macromolecules.

References and Notes

- H. K. Schachman, *Ultracentrifugation in Biochemistry* (Academic, New York, 1959).
- J. S. Johnson, G. Scatchard, K. A. Kraus, *J. Phys. Chem.* **63**, 787 (1959); E. G. Richards and H. K. Schachman, *ibid.*, p. 1578; H. K. Schachman, *Biochemistry* **2**, 887 (1963); H. K. Schachman, in *Ultracentrifugal Analysis in Theory and Experiment*, J. W. Williams, Ed. (Academic Press, New York, 1963), p. 171.
- K. V. Shooter and J. A. V. Butler, *Trans. Faraday Soc.* **52**, 734 (1956); V. N. Schumaker and H. K. Schachman, *Biochim. Biophys. Acta* **23**, 628 (1957).
- T. Svedberg and K. O. Pedersen, *The Ultracentrifuge* (Oxford Univ. Press, London, 1940).
- H. K. Schachman and S. J. Edelstein, *Biochemistry* **5**, 2681 (1966); I. Z. Steinberg and H. K. Schachman, *ibid.*, p. 3728, and references cited therein.
- R. Cohen, *Compt. Rend.* **256**, 3513 (1963); ——— and C. W. Hahn, *ibid.* **260**, 2077 (1965); R. Cohen, B. Giraud, A. Messiah, *Biopolymers* **5**, 203 (1967).
- J. Vinograd, R. Bruner, R. Kent, J. Weigle, *Proc. Nat. Acad. Sci. U.S.A.* **49**, 902 (1963).
- R. J. Britten and R. B. Roberts, *Science* **131**, 32 (1960); E. Burgi and A. D. Hershey, *Biophys. J.* **3**, 309 (1963).
- J. Vinograd, R. Radloff, R. Bruner, *Biopolymers* **3**, 481 (1965).
- F. W. Studier, *J. Mol. Biol.* **11**, 373 (1965).
- M. Gehatia and E. Katchalski, *J. Chem. Phys.* **30**, 1334 (1959); V. N. Schumaker and J. Rosenbloom, *Biochemistry* **4**, 1005 (1965); J. Vinograd and R. Bruner, *Biopolymers* **4**, 131, 1055 (1966); M. M. Rubin and A. Katchalski, *ibid.* **4**, 579 (1966).
- J. T. Edsall in *The Proteins*, H. Neurath and K. Bailey, Eds. (Academic Press, New York, ed. 1, 1953), vol. IB, p. 562.
- S. J. Edelstein and H. K. Schachman, *J. Biol. Chem.* **242**, 306 (1967).
- J. B. T. Aten and J. A. Cohen, *J. Mol. Biol.* **12**, 537 (1965); J. Hermans, Jr., and J. J. Hermans, *Koninkl. Ned. Adad. Wetenschap. Proc. Ser. B* **61**, 324 (1958); S. Claesson and U. Lohmander, *Makromol. Chem.* **17/19**, 310 (1956).
- B. H. Zimm and D. M. Crothers, *Proc. Nat. Acad. Sci. U.S.A.* **48**, 905 (1962).
- S. J. Gill and D. S. Thompson, *ibid.* **57**, 562 (1967).
- O. Quadrat and P. Munk, *Coll. Czech. Chem. Commun.* **30**, 3631 (1965); R. J. Douthart, unpublished work.
- V. N. Tsvetkov, in *Newer Methods of Polymer Characterization*, B. Ke, Ed. (Interscience, New York, 1964), p. 563; R. E. Harrington, in *Encyclopedia of Polymer Science and Technology*, N. M. Bikales, H. F. Mark, N. G. Gaylord, Eds. (Interscience, New York, 1967), vol. 7, p. 100.
- B. H. Zimm, *Rev. Sci. Instr.* **29**, 360 (1958); R. E. Harrington, *Biopolymers* **6**, 105 (1968).
- D. S. Thompson and S. J. Gill, *J. Chem. Phys.* **47**, 5008 (1968).
- P. J. Oriol and J. A. Schellman, *Biopolymers* **4**, 469 (1966).
- A. Wada and S. Kozawa, *J. Polymer Sci. A2*, 853 (1964); *J. Appl. Phys. Japan* **32**, 280 (1963); A. Wada, *Biopolymers* **2**, 361 (1964).
- S. Krause and C. T. O'Konski, *J. Amer. Chem. Soc.* **81**, 5082 (1959); *Biopolymers* **1**, 503 (1963); C. L. Riddiford and B. R. Jennings, *ibid.* **5**, 757 (1967).
- E. I. Golub, *Biopolymers* **2**, 113 (1964).
- A. Wada, in *Poly- α -Amino Acids*, G. D. Fasman, Ed. (Dekker, New York, 1967), p. 369.
- S. Takashima, *Biopolymers* **1**, 171 (1963); *ibid.* **4**, 663 (1966); *ibid.* **5**, 899 (1967); M. Hanss, *ibid.* **4**, 1035 (1966); M. Hanss and R. Banerjee, *ibid.* **5**, 879 (1967).
- G. Weber, *Advan. Protein Chem.* **8**, 415 (1953); ——— and F. W. J. Teale, in *The Proteins*, H. Neurath, Ed. (Academic Press, New York, ed. 2, 1965), vol. 3, p. 445; G. M. Edelman and W. O. McClure, *Accts. Chem. Res.* **1**, 65 (1968).
- C. W. Oseen, *Hydrodynamik* (Akademische Verlag, Leipzig, 1927).
- J. M. Burgers, in *2nd Report on Viscosity and Plasticity*, Amsterdam Acad. Sci. (Nordemann, New York, 1938), chap. 3.
- J. G. Kirkwood and J. Riseman, *J. Chem. Phys.* **16**, 565 (1948).
- J. G. Kirkwood, *Rec. Trav. Chim.* **68**, 649 (1949); *J. Polymer Sci.* **12**, 1 (1954); J. Riseman and J. G. Kirkwood, in *Rheology*, F. Eirich, Ed. (Academic Press, New York, 1956), vol. 1, p. 495.
- R. K. Dewan and K. E. Van Holde, *J. Chem. Phys.* **39**, 1820 (1963); R. D. Burkhart and J. C. Merrill, *ibid.* **46**, 4985 (1967).
- J. E. Hearst, *ibid.* **38**, 1062 (1963).
- V. A. Bloomfield, W. O. Dalton, K. E. Van Holde, *Biopolymers* **5**, 135 (1967); D. P. Filson and V. A. Bloomfield, *Biochemistry* **6**, 1650 (1967); *J. Polymer Sci. Ser. C*, in press.
- P. E. Rouse, Jr., *J. Chem. Phys.* **21**, 1272 (1953); F. Bueche, *ibid.* **22**, 603 (1954).
- B. H. Zimm, *ibid.* **24**, 269 (1956).
- P. J. Flory, *Principles of Polymer Chemistry* (Cornell Univ. Press, Ithaca, N.Y., 1953), p. 611.
- M. Kurata and H. Yamakawa, *J. Chem. Phys.* **29**, 311 (1958); O. B. Ptitsyn and Yu. E. Eizner, *Zh. Fiz. Khim.* **32**, 2464 (1958); *Zh. Tekhn. Fiz.* **29**, 1117 (1959); N. W. Tschoegl, *J. Chem. Phys.* **40**, 473 (1964).
- R. A. Harris and J. E. Hearst, *J. Chem. Phys.* **44**, 2595 (1966); J. E. Hearst, E. Beals, R. A. Harris, *ibid.*, in press.
- A. Peterlin, *J. Polymer Sci.* **5**, 473 (1950); *J. Chem. Phys.* **33**, 1799 (1960).
- M. Fixman, *J. Chem. Phys.* **42**, 3831 (1965); C. W. Pyun and M. Fixman, *ibid.*, p. 3838.
- A. Ishihara, *ibid.* **45**, 1855 (1966); **47**, 3821 (1967); *J. Polymer Sci. Ser. A-1* **5**, 2883 (1967); A. Ishihara and E. Guth, *J. Chem. Phys.* **46**, 4048 (1967).
- R. Zwanzig, J. Kiefer, G. H. Weiss, *Univ. of Maryland Inst. for Fluid Dynamics and Appl. Math. Tech Note BN-529* (1968).
- J. J. Erpenbeck and J. G. Kirkwood, *J. Chem. Phys.* **38**, 1023 (1963); R. Zwanzig, *ibid.* **45**, 1858 (1966).
- C. M. Tchen, *J. Appl. Phys.* **25**, 463 (1954).
- G. Weber, *Biochem. J.* **51**, 155 (1952); W. Harrington, P. Johnson, R. Ottewill, *ibid.* **62**, 569 (1956).
- G. Weber and L. B. Young, *J. Biol. Chem.* **239**, 1415, 1425 (1964).
- V. A. Bloomfield, *Biochemistry* **5**, 684 (1966).
- E. Mihalzi and W. F. Harrington, *Biochim. Biophys. Acta* **36**, 447 (1959); E. F. Woods, S. Himmelfarb, W. F. Harrington, *J. Biol. Chem.* **238**, 2374 (1963).
- M. E. Noelken, C. A. Nelson, C. E. Buckley, III, C. Tanford, *J. Biol. Chem.* **240**, 218 (1965); R. C. Valentine and N. M. Green, *J. Mol. Biol.* **27**, 615 (1967).
- E. F. J. van Bruggen, E. H. Wiebenga, M. Gruber, *J. Mol. Biol.* **4**, 1, 8 (1962); H. Fernandez-Moran, E. F. J. van Bruggen, M. Ohtsuki, *ibid.* **16**, 191 (1966).

52. K. E. Van Holde and L. B. Cohen, *Biochemistry* **3**, 1803, 1809 (1964); *Brookhaven Symp. Biol.* **17**, 184 (1964).
53. V. Bloomfield, K. E. Van Holde, W. O. Dalton, *Biopolymers* **5**, 149 (1967).
54. L. W. Nichol, J. L. Bethune, G. Kegeles, E. L. Hess, in *The Proteins*, H. Neurath, Ed. (Academic Press, New York, ed. 2, 1964), vol. 2, p. 305.
55. G. A. Gilbert, *Proc. Roy. Soc. London Ser. A* **250**, 377 (1959).
56. K. E. Van Holde, *J. Chem. Phys.* **37**, 1922 (1962); G. G. Belford and R. L. Belford, *ibid.*, p. 1926.
57. R. Josephs and W. F. Harrington, *Proc. Nat. Acad. Sci. U.S.* **58**, 1587 (1967).
58. G. Kegeles, L. Rhodes, J. L. Bethune, *ibid.*, p. 45; L. F. Ten Eyck and W. Kauzmann, *ibid.*, p. 888.
59. J. C. Gerhart and H. K. Schachman, *Biochemistry* **7**, 538 (1968).
60. J. Eigner and P. Doty, *J. Mol. Biol.* **12**, 549 (1965).
61. D. M. Crothers and B. H. Zimm, *ibid.*, p. 525.
62. H. B. Gray, Jr., V. A. Bloomfield, J. E. Hearst, *J. Chem. Phys.* **46**, 1493 (1967); P. Sharp and V. A. Bloomfield, *ibid.* **48**, 2149 (1968).
63. O. Kratky and G. Porod, *Rec. Trav. Chim.* **68**, 1106 (1949).
64. R. J. Douthart and V. A. Bloomfield, *Biopolymers*, in press.
65. J. Harpst, A. Krasna, B. H. Zimm, *Biopolymers* **6**, 595 (1968); P. Sharp and V. A. Bloomfield, *ibid.*, in press; E. P. Geiduschek and A. Holtzer, *Advan. Biol. Med. Phys.* **6**, 431 (1958).
66. R. E. Harrington, *Biopolymers* **6**, 105 (1968).
67. For extensive references, see J. Vinograd and J. Lebowitz, *J. Gen. Physiol.* **49**, 103 (1966); V. A. Bloomfield, *Macromol. Rev.*, in press.
68. V. A. Bloomfield and B. H. Zimm, *J. Chem. Phys.* **44**, 315 (1966); M. Fukatsu and M. Kurata, *ibid.*, p. 4539.
69. J. Vinograd, J. Lebowitz, R. Radloff, R. Watson, P. Laipis, *Proc. Nat. Acad. Sci. U.S.* **53**, 1104 (1965).
70. H. B. Gray, Jr., *Biopolymers* **5**, 1009 (1967).
71. D. A. Clayton and J. Vinograd, *Nature* **216**, 652 (1967); I. B. Dawid and D. R. Wolstenholme, *J. Mol. Biol.* **28**, 233 (1967).
72. J. C. Wang, D. Baumgarten, B. M. Olivera, *Proc. Nat. Acad. Sci. U.S.* **58**, 1852 (1967).
73. S. Brenner, G. Streisinger, R. W. Horne, S. P. Champe, L. Barnett, S. Benzer, M. W. Rees, *J. Mol. Biol.* **1**, 281 (1959).
74. A. E. Hook, D. Beard, A. R. Taylor, D. G. Sharp, J. W. Beard, *J. Biol. Chem.* **165**, 241 (1946); D. G. Sharp, A. E. Hook, A. R. Taylor, D. Beard, J. W. Beard, *ibid.*, p. 259.
75. M. F. Maestre, *Polymer Preprints* **7**, 1163 (1966).
76. I. J. Bendet, J. L. Allison, M. A. Lauffer, *Virology* **6**, 571 (1958); I. J. Bendet, L. G. Swaby, M. A. Lauffer, *Biochim. Biophys. Acta* **25**, 252 (1957); M. A. Lauffer and I. J. Bendet, *ibid.* **55**, 211 (1962).
77. D. J. Cummings and L. M. Kozloff, *Biochim. Biophys. Acta* **44**, 445 (1960); *J. Mol. Biol.* **5**, 50 (1962); D. J. Cummings, *Biochim. Biophys. Acta* **68**, 472 (1963).
78. D. P. Filson and V. A. Bloomfield, *Biochemistry* **6**, 1650 (1967); D. P. Filson, thesis, University of Illinois (1967).
79. L. C. Kanner and L. M. Kozloff, *Biochemistry* **3**, 215 (1964).
80. R. J. Douthart and V. A. Bloomfield, unpublished results.
81. P. Pfuderer, P. Cammarano, D. R. Holladay, G. D. Novelli, *Biochim. Biophys. Acta* **109**, 595 (1965).
82. D. P. Filson and V. A. Bloomfield, *ibid.* **155**, 169 (1968).
83. Preparation of this article was supported in part by PHS research grant GM 12555-04.

Eye Movement Control in Primates

The oculomotor system contains specialized subsystems
for acquiring and tracking visual targets.

David A. Robinson

The retinas of most animals in which the eyes face forward have a special area, the fovea centralis, which has a high density of photoreceptors. To see an object with good visual acuity, these animals must move their eyes to place its image on each fovea. The eye movement system is especially well developed in primates. The purpose of this system is to acquire a visual target and then track it so that its image remains on the fovea. To do this, the oculomotor system overcomes, with nervous tissue and muscle, the same problems encountered in tracking systems designed by man. Current research in this field is directed not only toward diagnosis of eye movement disorders in man but also toward understanding

how the central nervous system processes information and manipulates signals to achieve the regulation and coordination which this control system displays.

Four Oculomotor Subsystems

All tracking systems made by man or nature have at least two requirements: to acquire a given target rapidly, and then to follow it if it moves relative to the environment. The eye movement systems which perform these two functions are called the saccadic and smooth pursuit systems. When the tracking device is mounted on a moving platform (for example, a shipboard-mounted radar system) an additional requirement is that of stabilizing the tracking device automatically against movements of the platform. For eye

movements, this function is fulfilled by the vestibular system. Finally, for depth perception (analogous to stereoscopic range-finding in some gunnery systems) the vergence system controls the degree of convergence of the visual axes of the eyes necessary to maintain the target image on each fovea. In short, the saccadic, smooth pursuit, vestibular, and vergence systems perform the four functions of acquiring targets, tracking them if they move in the environment, compensating for movements of the head in the environment, and tracking in depth.

Almost all eye movements in primates are combinations of the movements produced by each of these subsystems. The tasks are different from each other and appear to be performed by separate neurological control systems specializing in individual tasks. They can be excited independently, and their responses can be observed independently, so that each may be studied in isolation. Figure 1 illustrates this subdivision and the types of movements produced by each system. Except for the vestibular system, which obtains information about movement of the head in space from the semicircular canals, all the systems depend on visual information derived from the retina and carried centrally on the optic nerve. The outputs of the four systems converge on the motor nuclei whose motor cells relay the information along the motor nerves to the extraocular muscles. Each eye is equipped with three pairs of antagonist muscles that rotate the globe in three roughly mutually perpendicular planes: horizontal, vertical, and torsional. This arrange-

The author is an associate professor in the Division of Biomedical Engineering, Department of Medicine of the Johns Hopkins School of Medicine, Baltimore, Maryland.